Mechanisms of the Enhanced Antibacterial Effect of Ag-TiO2 Coatings

Liu, Chen; Geng, Lei; Yu, YiFan; Zhang, Yutong; Zhao, Buyun; Zhao, Qi

Published in:
Biofouling

DOI:
10.1080/08927014.2017.1423287

Publication date:
2018

Document Version
Publisher's PDF, also known as Version of record

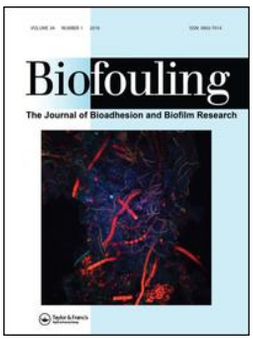

Taylor & Francis
Taylor & Francis Group

Biofouling
The Journal of Bioadhesion and Biofilm Research

ISSN: 0892-7014 (Print) 1029-2454 (Online) Journal homepage: http://www.tandfonline.com/loi/gbif20

Mechanisms of the enhanced antibacterial effect of Ag-TiO_2 coatings

Chen Liu, Lei Geng, YiFan Yu, Yutong Zhang, Buyun Zhao & Qi Zhao

To cite this article: Chen Liu, Lei Geng, YiFan Yu, Yutong Zhang, Buyun Zhao & Qi Zhao (2018): Mechanisms of the enhanced antibacterial effect of Ag-TiO_2 coatings, Biofouling, DOI: 10.1080/08927014.2017.1423287

To link to this article: https://doi.org/10.1080/08927014.2017.1423287

Published online: 29 Jan 2018.

BIOFOULING, 2018
https://doi.org/10.1080/08927014.2017.1423287

Taylor & Francis
Taylor & Francis Group

Mechanisms of the enhanced antibacterial effect of Ag-TiO_2 coatings

Chen Liu[a], Lei Geng[a], YiFan Yu[a], Yutong Zhang[a], Buyun Zhao[b] and Qi Zhao[c]

[a]Department of Chemistry, School of Pharmaceutical Science, Capital Medical University, Beijing, PR China; [b]Medical Research Council Laboratory of Molecular Biology, University of Cambridge, Cambridge, UK; [c]Division of Mechanical Engineering, University of Dundee, Dundee, UK

ABSTRACT

It has been demonstrated that Ag-TiO_2 nanocomposite coatings with excellent antimicrobial activity and biocompatibility have the potential to reduce infection problems. However, the mechanism of the synergistic effect of Ag-TiO_2 coatings on antibacterial efficiency is still not well understood. In this study, five types of Ag-TiO_2 nanocomposited coatings with different TiO_2 contents were prepared on a titanium substratum. Leaching tests indicated that the incorporation of TiO_2 nanoparticles into an Ag matrix significantly promoted Ag ion release. Surface energy measurements showed that the addition of TiO_2 nanoparticles also significantly increased the electron donor surface energy of the coatings. Bacterial adhesion assays with *Escherichia coli* and *Staphylococcus aureus* demonstrated that the number of adhered bacteria decreased with increasing electron donor surface energy. The increased Ag ion release rate and the increased electron donor surface energy contributed to an enhanced antibacterial efficiency of the coatings.

ARTICLE HISTORY
Received 21 October 2017
Accepted 26 December 2017

KEYWORDS
Bacterial adhesion; surface energy; coatings; medical implants; infection

1. Introduction

Titanium (Ti) and its alloys are widely used in both orthopedic and dental implants (Jia et al. 2016). However, microbial colonization and biofilm formation on the implanted devices represent an important complication in orthopedic and dental surgery and may result in implant failure (De Giglio et al. 2013). Silver has been known as a broad-spectrum bactericide for centuries. It has been demonstrated that silver nanoparticle coatings on Ti based implants increased their biocompatibility and antibacterial properties (Gyorgyey et al. 2016; Sulej-Chojnacka et al. 2016). Titanium dioxide (TiO_2) has also been known as a broad-spectrum bactericide for a long time. Matsunaga et al. (1985) first reported the microbiocidal effect of TiO_2 photocatalytic reactions. The antibacterial mechanism of TiO_2 has been proven to involve oxidation of all organic compounds in the microorganisms by the generated reactive oxygen species which leads to cell death (Kim et al. 2014; Motlagh et al. 2014). In addition, TiO_2 with moderate hardness and excellent resistance to wear and corrosion can significantly accelerate osteoblast cell growth and improve bone-forming functionality and direct the fate of stem cells in orthopedic-associated implants (Frandsen et al. 2013; Li et al. 2015). This suggests that a Ag-TiO_2 nanocomposite coating may offer a promising solution for improvement of the antibacterial properties of dental and orthopedic implants (Cotolan et al. 2016; Gyorgyey et al. 2016). It has been reported that Ag-TiO_2 nanocomposite coatings exhibit a synergistic effect on antibacterial activity, which made their bactericidal activities stronger than Ag or TiO_2 coatings (Ashkarran et al. 2011; Esfandiari et al. 2014; Motlagh et al. 2014; Prakash et al. 2016). The enhanced antibacterial effect was explained by a contact killing action mechanism (Prakash et al. 2016) and the bactericidal capacity was found to depend on the size characteristics of the Ag-TiO_2 coatings (Esfandiari et al. 2014). It was also reported that Ag-TiO_2 nanoparticles extended the light absorption spectrum toward the visible region and significantly enhanced the inactivation of bacteria under visible light irradiation due to the effect of Ag, by acting as electron traps in the TiO_2 band gap (Ashkarran et al. 2011). However, the mechanism of the enhanced antibacterial effect of the Ag-TiO_2 coatings is still not well understood. The aim of the present work was therefore to investigate the mechanism of the synergistic effect of Ag-TiO_2 coatings on their antibacterial properties. For this purpose, a range of novel Ag-TiO_2 nanocomposite coatings with different TiO_2 content on a titanium substratum were prepared using an electroless plating technique, and the antibacterial

CONTACT Qi Zhao Q.Zhao@dundee.ac.uk

performance of the coatings was evaluated using two types of bacteria, ie the Gram-negative *Escherichia coli* and the Gram-positive *Staphylococcus aureus*.

2. Materials and methods

2.1. Preparation of Ag-TiO_2 coatings

A range of Ag-TiO_2 nanocomposite coatings were prepared on a substratum of pure Ti disks 10 mm in diameter. The disks were first cleaned ultrasonically with acetone, ethyl alcohol and deionized water respectively for 5 min, then they were further treated by alkaline cleaning for 5 min and pickling cleaning for 5 min. The alkaline cleaning solution comprised NaOH 25 g l^{-1}, Na_3PO_4 30 g l^{-1}, Na_2CO_3 25 g l^{-1} and Na_2SiO_3 10 g l^{-1}, and the pickling solution was HCl 30%: H_2O (1:1 in volume). After this, both sides of the disks were irradiated with UV light at 385 nm for 2 h to activate the inert Ti surfaces, then the disks were immersed in a coupling agent solution for 2 h in order to create the reactive surfaces using the method described previously (Guo et al. 2015). TiO_2 powder with a particle size of 25 nm (Sigma-Aldrich, Dorset, UK) was used. Five types of Ag-TiO_2 coatings with the different TiO_2 concentrations in the plating solution (0.1, 0.3, 0.5, 1.5 and 2 g l^{-1}) were prepared by an electroless plating technique under dark conditions. An Ag coating was also prepared for comparison. The composition of the plating bath and operating conditions are presented in Table 1. All the samples were sterilized in an autoclave at 120°C for 15 min before bacterial adhesion assays.

2.2. Characterization of the Ag-TiO_2 coatings

The surface morphologies of the pure Ti, Ag and Ag-TiO_2 coatings were observed by scanning electron microscopy (SEM) (S-4800, Hitachi, Hitachinaka, Japan). The elemental composition and distribution of Ag and TiO_2 were determined by energy dispersive X-ray analysis (EDX) (EMAX350, Horiba, Kyoto, Japan). The surface topographic and roughness of coatings were observed by atomic force microscopy (AFM) (Multimode 8, Bruker, Karlsruhe, Germany) with tip scanning. Their phase compositions were analyzed by X-ray diffraction XRD (D8 Advance, Bruker, Karlsruhe, Germany). The bonding states of the surface constituents were identified by X-ray photoelectron spectroscopy XPS (ESCALAB 250, Thermo Fisher Scientific, Waltham, MA, USA).

Table 1. Plating bath composition and operating conditions for electroless Ag coating and Ag-TiO_2 nano-composite coatings.

Composition	Ag	Ag-TiO_2
$AgNO_3$ (g l^{-1})	2–7	2–7
NaOH (g l^{-1})	1.5–5	1.5–5
$NH_3{\cdot}H_2O$ (ml l^{-1})	100–150	100–150
$C_6H_{12}O_6$ (g l^{-1})	3.6–7.2	3.6–7.2
$C_4H_6O_4$	Trace	Trace
TiO_2 (g l^{-1})	0	0.1–2
Temperature (°C)	25	25
Stirring(rpm)	0	40

2.3. Ion release

The amounts of Ag and Ti ions released from the coatings were monitored by soaking them in PBS at a pH of 7.3 ± 0.1. The tested samples were immersed in a sealed tank containing 25 ml of PBS and kept at 37°C at 150 rpm. The releases of Ag and Ti ions from the different coatings in PBS were determined by inductively coupled plasma atomic emission spectrometry ICP-AES (Varian 710-ES, Agilent Technologies, Palo Alto, CA, USA) with immersion times of 1 h, 24 h, three days and seven days, respectively, which was the same time as used for bacterial adhesion assays, as described below.

2.4. Contact angle and surface energy

After exposure to UV light, the contact angles of the coatings were measured with a Dataphysics OCA-20 contact angle analyzer (DataPhysics Instruments GmbH, Filderstadt, Germany). The test liquids used for contact angle measurements were distilled water (W), diiodomethane (Di) and ethylene glycol (EG), respectively. The contact angles of living biofilms of *E. coli* and *S. aureus* used for bacterial adhesion assays were also measured by the sessile drop method. Details of the contact angle measurements and surface energy calculation are described in previous study (Liu and Zhao 2011). The surface energies of coatings were calculated using the van Oss (1994) approach, including the Lifshitz-van der Waals (LW) apolar component (γ_2^{LW}), the Lewis acid/base polar component (γ_2^{AB}), the electron donor component (γ_2^-) and the electron acceptor (γ_2^+) component. The ratio of γ_2^{LW}/γ_2^- (also known as the CQ ratio) was also calculated to determine the adhesion strength (Liu and Zhao 2011).

2.5. Bacterial adhesion and removal

E. coli ATCC 8739 and *S. aureus* ATCC 6538 were used for bacterial adhesion and removal assays on the Ag-TiO_2 coatings. The pure Ti and Ag coatings were also evaluated for comparison. After the frozen bacterial stocks had been defrosted, they were cultured in tryptone soya agar (TSA) plates in an incubator overnight at 37°C. A single colony was taken into 10 ml of tryptic soy broth (TSB) and grown statically overnight at 37°C. Then, 500 µl of each bacterial suspension were transferred into 100 ml of the corresponding medium in a conical flask and cultured

in a shaker-incubator (LUXI SZX-IS1A, Beijing, China) at 150 rpm at 37°C until the bacteria had grown to mid-exponential phase. Then, the suspensions with 10^7 CFU ml^{-1} of each type of bacterium were prepared. For bacterial adhesion assays, each sample was immersed in a tank containing 25 ml of bacterial suspension at 37°C for 1 h, 24 h, three days and seven days, respectively. After that, each sample was moved up and down vertically for 25 s in a glass tank containing 50 ml of distilled water at a constant speed 0.028 m s^{-1} with a corresponding shear stress of 0.014 N m^{-2} in order to remove adhered bacteria using a home-made dipping device. Then, the total number of adhered bacteria and the bacterial removal rate for each sample were determined on TSA plates by a viable plate counting method. Details of the bacterial the adhesion assay are described in a previous study (Liu and Zhao 2011).

2.6. Statistical analysis

For the bacterial adhesion assay five replicate samples of each coating were tested, and for each sample three measurements were performed ($N = 15$). One-way analysis of variance (ANOVA) was used to determine whether there were any statistically significant differences between the means of two or more independent groups. If $p < 0.05$ they are considered to be significantly different.

3. Results

3.1. Surface characterizations

Figure 1a shows a typical SEM image of pure Ti with gullied surface and Figure 1b shows the morphology of an Ag coating with typical polygonal rounded hillock units. The morphology of Ag-TiO_2 coating has a similar structure to the Ag coating in Figure 1c, which was produced with 1.5 g l^{-1} TiO_2 in the plating solution. Clearly, the TiO_2 particles were homogenously incorporated in the Ag matrix.

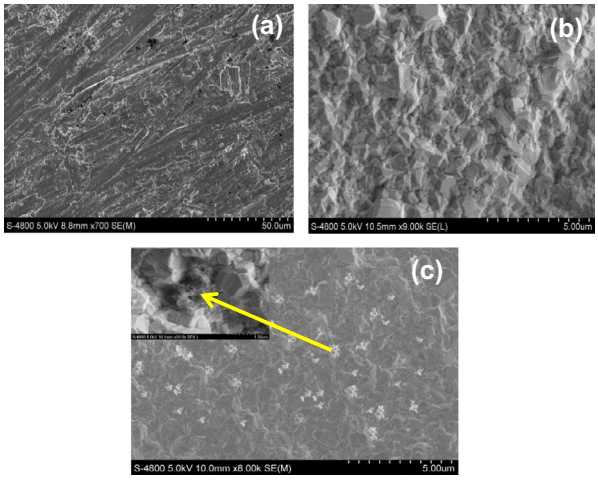

Figure 1. Typical SEM images of samples: (a) Ti; (b) Ag coating, (c) Ag-TiO_2 coating.

The Ag and TiO_2 contents on the coatings were determined by EDX analysis based on their Ti, O and Ag contents. Figure 2a and b show the EDX images of the Ag coating and the Ag-TiO_2 coating (1.5 g l^{-1} TiO_2), respectively. The detailed EDX results for all the coatings are given in Table 2, which indicates that TiO_2 was embedded into the Ag-based matrix. Furthermore, the results demonstrate that the TiO_2 content in the Ag-TiO_2 coatings increased with increasing TiO_2 concentration in the plating solution, while the Ag content on the Ag-TiO_2 coatings decreased with increasing TiO_2 concentration in the plating solution.

Figure 3 shows the surface morphology of the pure Ti, and Ag coatings and the Ag-TiO_2 coating (1.5 g l^{-1} TiO_2, see Table 2) by AFM, respectively. The roughness for each surface was an average of six measurements at different position with the surface area of 10 × 10 μm^2. The surface roughness values (*Ra*) of the Ag and Ag-TiO_2 coatings were in the range of 102–125 (±14) nm, while the *Ra* values for the pure Ti were ~202 ± 23 nm (see Table 2). The AFM images indicated that the roughness of the pure Ti disk was higher than that of the Ag coating and the Ag-TiO_2 coatings.

Figure 4 shows the typical XRD spectra of the pure Ti, Ag and Ag-TiO_2 coatings (TiO_2 1.5 g l^{-1}). It can be seen that the pure Ti surface only contained the Ti phase, while the pattern of the Ag coating contained the silver phase and small peaks of Ti from the substratum. The Ag-TiO_2 coating showed Ag and anatase TiO_2 peaks, and some small peaks of the rutile phase, which is consistent with the results of Prakash et al. (2016). Clearly the Ag-TiO_2 coating was composed of Ag and TiO_2 phases.

Further XPS studies revealed that Ag, Ti and O peaks were found for all the Ag-TiO_2 coatings. Figure 5 shows the results for the typical Ag-TiO_2 (TiO_2 0.5 g l^{-1}) coating. The peaks of Ag 3d, Ti 2P and O1s were clearly observed (Figure 5a). The C1s signal was caused by surface contamination. The XPS spectra of elemental Ag from the coating shows the energies of Ag 3d peaks at 368.2 eV and 374.2 eV, respectively, which fits with Ag^0 in the coating (Figure 5b). The bonding energy of the Ti 2p peak is located at 458.8 eV and 464.6 eV (Figure 5c) and O1s peak is located at 529.9 eV (Figure 5d), which are attributed to the chemical bonding of TiO_2. The Ti 2p and O1s peak structures become broader and much slighter in asymmetries due to the amount of Ag in the coatings. All the XPS binding energies of the Ag 3d, Ti 2P and O1s photoelectrons for the coatings are consistent with the results of Kuo et al. (2007). The results

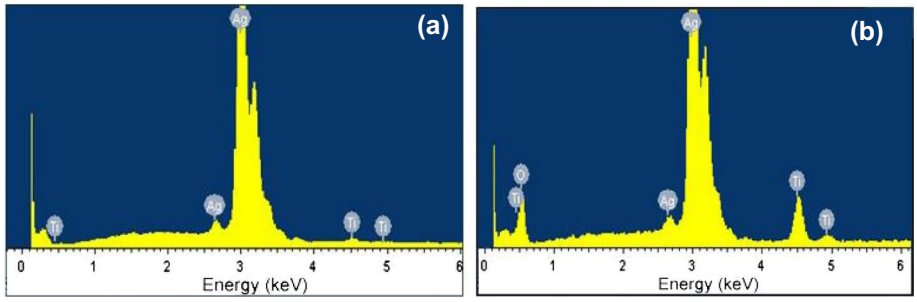

Figure 2. Typical EDX images of samples: (a) Ag coating, (b) Ag-TiO_2 coating.

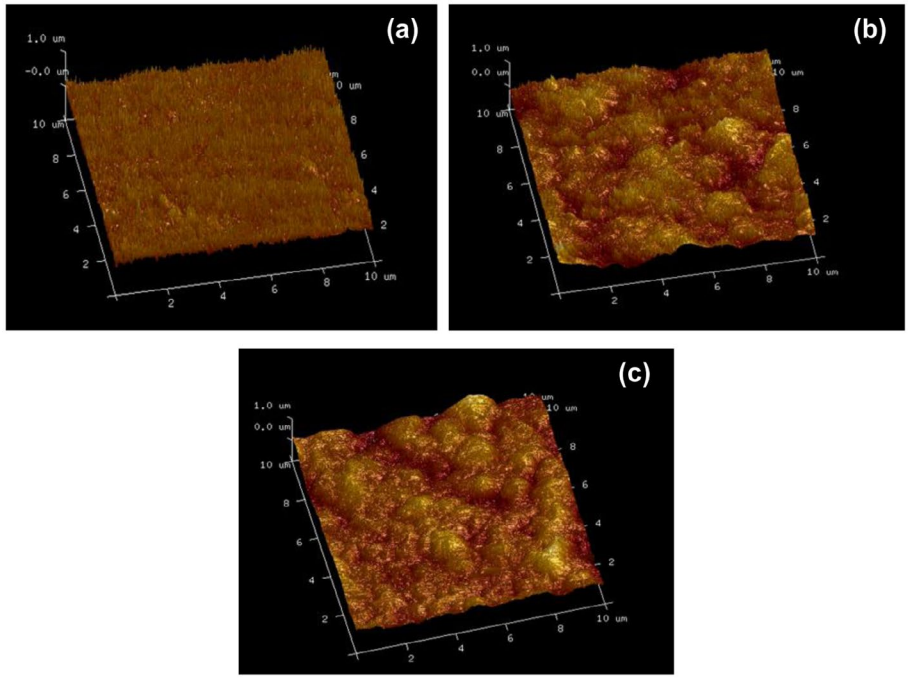

Figure 3. AFM images of samples: (a) Ti, (b) Ag coating, (c) Ag-TiO_2 coating.

Table 2. Elemental composition and roughness results.

Sample	TiO_2 concentration in solution (g l^{-1})	Elemental composition (wt%)			Roughness (nm)
		O	Ti	Ag	
Ti	–	–	–	–	202 ± 23
Ag	–	0	1.06	98.94	115 ± 10
Ag-TiO_2 1	0.1	1.65	1.44	96.91	117 ± 13
Ag-TiO_2 2	0.3	2.14	1.83	96.03	118 ± 7.0
Ag-TiO_2 3	0.5	10.11	2.89	87.00	113 ± 16
Ag-TiO_2 4	1.5	17.18	5.73	77.09	110 ± 6.0
Ag-TiO_2 5	2	18.95	7.61	73.44	102 ± 11

indicate that the TiO_2 nano-particles were embedded in the Ag-based coating. The XPS peaks were in agreement with EDX and XRD results, which demonstrate that the Ag-TiO_2 coatings were successfully prepared on the Ti substratum.

3.2. Ion release

The amounts of Ag ion released from the Ag-TiO_2 coatings (with TiO_2 0.1, 0.3, 0.5, 1.5 and 2.0 g l^{-1}, respectively) in PBS are given in Table 3. The amount of Ag ion released from the Ag coatings increased steadily to

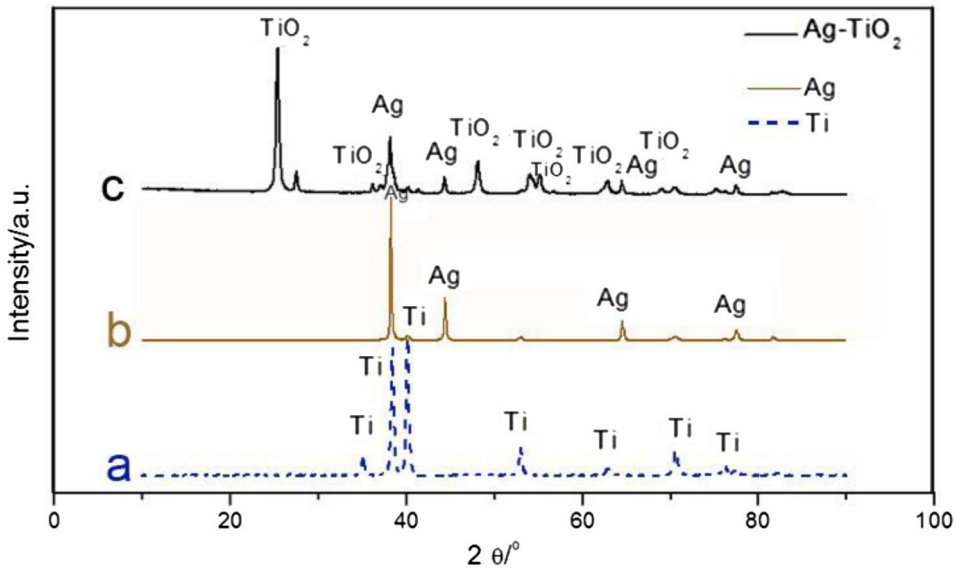

Figure 4. XRD patterns of samples: (a) Ti, (b) Ag coating, (c) Ag-TiO_2 coating.

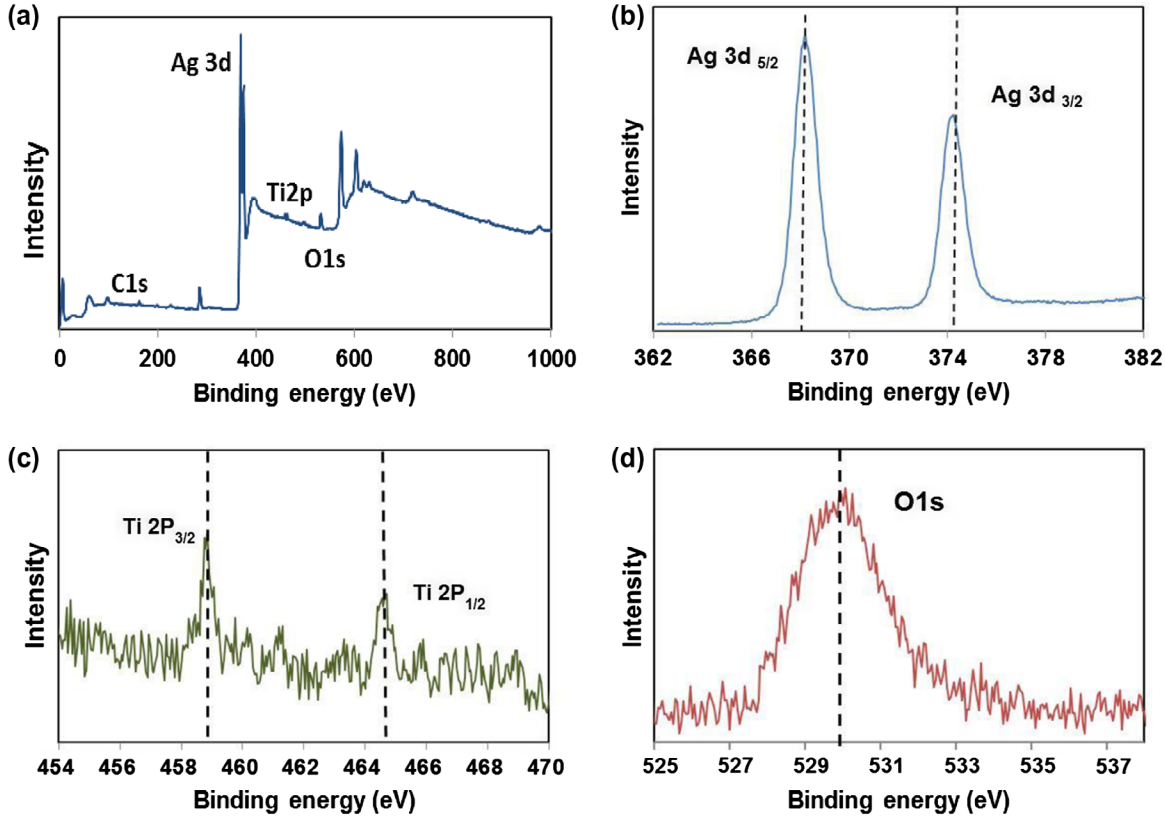

Figure 5. XPS spectra of a Ag-TiO_2 coating (TiO_2: 0.5 g l^{-1}).

0.5811 ± 0.0155 ppm cm^{-2} from 0.1276 ± 0.0010 ppm cm^{-2} during the 7 days while the amount of Ag ion released from Ag-TiO_2 coatings increased from 0.2404±0.0011 ppm cm^{-2} to 0.6281±0.0104 ppm cm^{-2}. The results indicate that in general the amounts of Ag ion released from all the Ag-TiO_2 coatings were much higher than that released from the Ag coating. Clearly, the incorporation of TiO_2 nanoparticles into the Ag coating promoted Ag ion release.

3.3. Contact angles and surface energy

Table 4 shows the contact angles and surface energies of the coatings used in this study, including pure Ti, the Ag coating and the Ag-TiO_2 coatings with different TiO_2 contents. The results show that the water contact angle of the Ag-TiO_2 coatings was slightly lower than that of Ti or Ag coatings due to the incorporation of TiO_2 nanoparticles. Previous studies reported that the water contact angle on TiO_2-coated surfaces significantly decreased after exposure to UV light (Li and Logan 2005; Liu and Zhao 2011). Table 4 indicates that, in general, the electron donor surface energy (γ_2^-) of the Ag-TiO_2 coatings increased with increasing TiO_2 concentrations in the plating solution or the TiO_2 contents in the coatings. It was found that the ratio of LW apolar to the electron donor surface energy components of the substrata (γ_2^{LW}/γ_2^- or CQ ratio) significantly decreased with increasing TiO_2 concentration in the plating solution. However, no correlation was observed between other surface energy components of the coatings (γ_2^{LW},γ_2^+, γ_2^{AB} or γ_2^{TOT}) and TiO_2 concentration in the plating solution. The contact angles and surface energy of the *E. coli* and *S. aureus* used in this study are also given in Table 4. *S. aureus* exhibits a more hydrophilic surface and a higher value of electron donor surface energy (γ_2^-), compared to *E. coli*.

3.4. Bacterial adhesion assays

In order to compare the antibacterial properties of the Ti surface, the Ag coating and the Ag-TiO_2 coatings, *E. coli* and *S. aureus* were used for adhesion assays with contact times of 1, 24, 72 and 168 h, respectively. The Ag-TiO_2 coatings performed best against bacterial adhesion compared with the Ti surface and the Ag coating at different contact times. Figure 6 shows typical results for the contact time 168 h. The Ag-TiO_2 coatings reduced adhesion of *E. coli* by up to 52.4% ($p < 0.05$) and 39.8% ($p < 0.05$), respectively, compared with the Ti surface and the Ag coating (Figure 6a). The Ag-TiO_2 coatings reduced the adhesion of *S. aureus* by up to 45.1% ($p < 0.05$) and 41.2%

Table 3. Comparison of the amount of Ag ion released (ppm cm^{-2}).

Time (h)	Ag coating	Ag-TiO_2 1	Ag-TiO_2 2	Ag-TiO_2 3	Ag-TiO_2 4	Ag-TiO_2 5
1	0.1276 ± 0.0010	0.2404 ± 0.0008	0.2404 ± 0.0003	0.2404 ± 0.0003	0.2404 ± 0.0005	0.2404 ± 0.0011
24	0.2893 ± 0.0057	0.3474 ± 0.0092	0.2590 ± 0.0067	0.2712 ± 0.0127	0.3030 ± 0.0162	0.3243 ± 0.0199
48	0.3562 ± 0.0112	0.3896 ± 0.0220	0.3498 ± 0.0322	0.3775 ± 0.0188	0.4167 ± 0.0130	0.3880 ± 0.0244
72	0.4341 ± 0.0125	0.4456 ± 0.0176	0.4568 ± 0.0193	0.4584 ± 0.0096	0.4804 ± 0.0141	0.4819 ± 0.0081
168	0.5811 ± 0.0155	0.6281 ± 0.0104	0.5951 ± 0.0174	0.6021 ± 0.0099	0.6244 ± 0.0081	0.6263 ± 0.0110

Table 4. Contact angle and surface energy components of the coating samples and bacteria.

Sample	TiO_2 concentration in solution (g l^{-1})	Contact angle, θ (°)			Surface free energy (mJ m^{-2})					CQ ratio γ^{LW}/γ^-
		θ^W	θ^{Di}	θ^{EG}	γ^{LW}	γ^+	γ^-	γ^{AB}	γ^{TOT}	
Ti		79.2 ± 1.5	60.0 ± 0.3	37.1 ± 0.5	28.58	2.92	3.64	6.52	35.09	7.85
Ag	0	73.7 ± 1.2	48.5 ± 0.6	46.9 ± 1.1	35.11	0.36	9.93	3.79	38.90	3.53
Ag-TiO_2 1	0.1	62.8 ± 2.2	42.4 ± 1.0	38.9 ± 1.2	38.38	0.24	18.33	4.22	42.61	2.09
Ag-TiO_2 2	0.3	68.1 ± 3.1	46.3 ± 1.4	47.8 ± 2.1	36.31	0.09	16.15	2.47	38.78	2.25
Ag-TiO_2 3	0.5	70.7 ± 2.5	54.0 ± 0.9	57.0 ± 0.6	32.02	0.01	18.12	0.87	32.89	1.77
Ag-TiO_2 4	1.5	61.4 ± 0.5	45.9 ± 0.2	53.3 ± 1.5	36.53	0.05	28.04	2.38	38.91	1.30
Ag-TiO_2 5	2	57.8 ± 1.4	63.3 ± 0.5	32.0 ± 0.3	26.68	2.06	23.42	13.88	40.56	1.14
E. coli		65.4	60.8	13.2	28.11	4.39	10.31	12.9	41.57	
S. aureus		54.2	40.6	20.4	37.37	0.88	21.33	8.68	46.05	

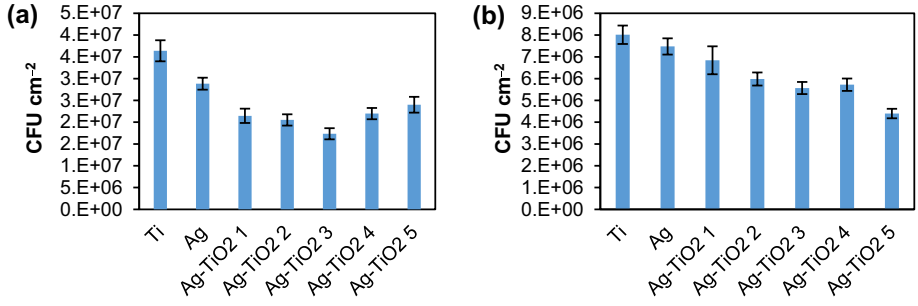

Figure 6. Comparison of the antibacterial performance of a Ti surface, an Ag coating and an Ag-TiO_2 coating with (a) *E. coli* and (b) *S. aureus* (N=15, error bars = SE).

($p < 0.05$), respectively, compared with the Ti surface and the Ag coating (Figure 6b).

In order to observe bacterial adhesion behavior on the different substrata, the Ti disks and the Ag-TiO_2 coatings were observed with SEM after immersion in the suspensions of *E. coli* and *S. aureus* for 24 h. Figure 7a and b show typical SEM images of *E. coli* adhered on the pure Ti disk and the Ag-TiO_2 coating, respectively. A large number of the rod-shaped *E. coli* cells formed on the Ti surface with a size of ~4 μm × 0.3 μm (Figure 7a); while a few *E. coli* cells formed on the Ag-TiO_2 surface with a size of ~1 μm × 0.3 μm (Figure 7b). Figure 7c shows that a large number of spherical *S. aureus* cells formed on the pure Ti and Figure 7d shows a few *S. aureus* cells formed on the Ag-TiO_2 coating. These results indicate that the cells did not prefer to attach to the Ag-TiO_2 coatings compared to the Ti surface.

3.5. Bacterial removal assays

The experimental results showed that the removal rates of *E. coli* and *S. aureus* from the Ag and the Ag-TiO_2 coatings were higher than that from the pure Ti surface ($p < 0.05$) due to the bactericidal properties of the Ag and the Ag-TiO_2 coatings. Figure 8 shows a comparison of the Ti, the Ag and the Ag-TiO_2 coatings (TiO_2: 1.5 g l^{-1}) on bacterial removal rates at the contact times of 1, 24, 72 and 168 h, respectively. Figure 8a also indicates that the *E. coli* removal rate increased to the highest amount (89.0% ± 6.5) when the contact time reached 72 h ($p < 0.05$). Similar results were obtained for *S. aureus* (Figure 8b).

3.6. Effect of surface energy on bacterial adhesion and removal

Figure 9a and c show the influence of the electron donor surface energy (γ_2^-) of the seven surfaces (see Table 4) on the adhesion of *E. coli* and *S. aureus* cells for the contact times of 1, 24, 72 and 168 h, respectively. The number of adhered bacteria decreased with increasing the γ_2^- surface energy of the coatings. The correlation coefficient R^2 values were in the range of 0.71–0.85. Figure 9b and d show that the number of adhered bacteria increased with increasing the γ_2^{LW}/γ_2^- ratio (CQ ratio). The results indicate that there was a good correlation between bacterial adhesion and the γ_2^{LW}/γ_2^- ratio. The correlation coefficient R^2 values were in the range of 0.72–0.91.

Figure 10a and c show the effect of the γ_2^- values of the coatings on the removal of *E. coli* and *S. aureus* biofilms

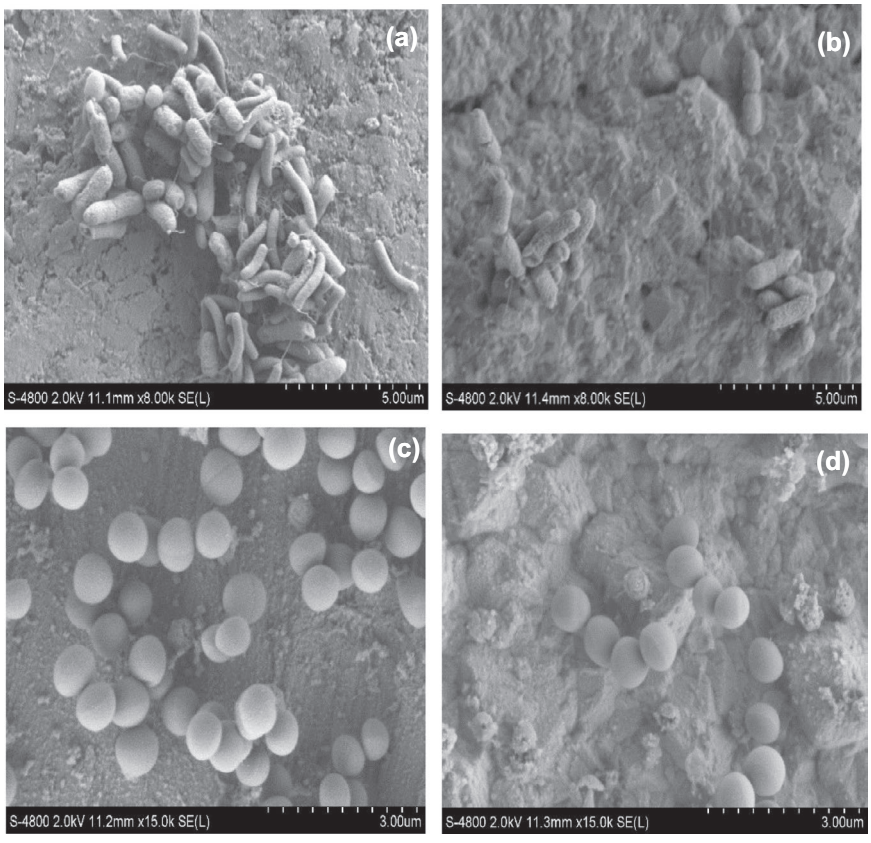

Figure 7. Typical SEM images of (a) *E. coli* on a Ti surface, (b) *E. coli* on an Ag-TiO_2 coating, (c) *S. aureus* on a Ti surface and (d) *S. aureus* on an Ag-TiO_2 coating.

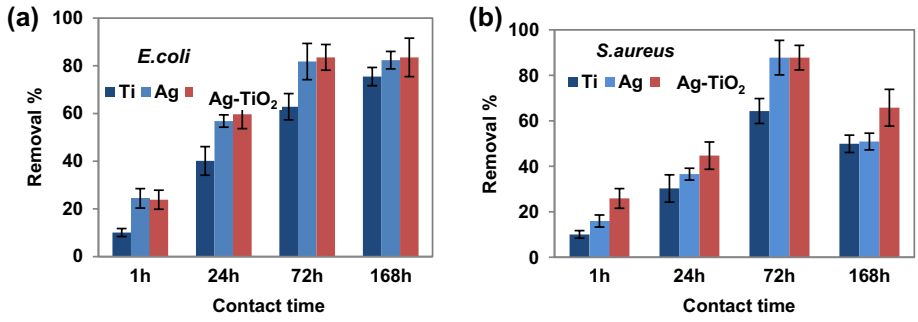

Figure 8. Comparison of bacterial removal from Ti surface, Ag coating and Ag-TiO_2 coating with (a) *E. coli* and (b) *S. aureus* (N=15, error bars are standard error).

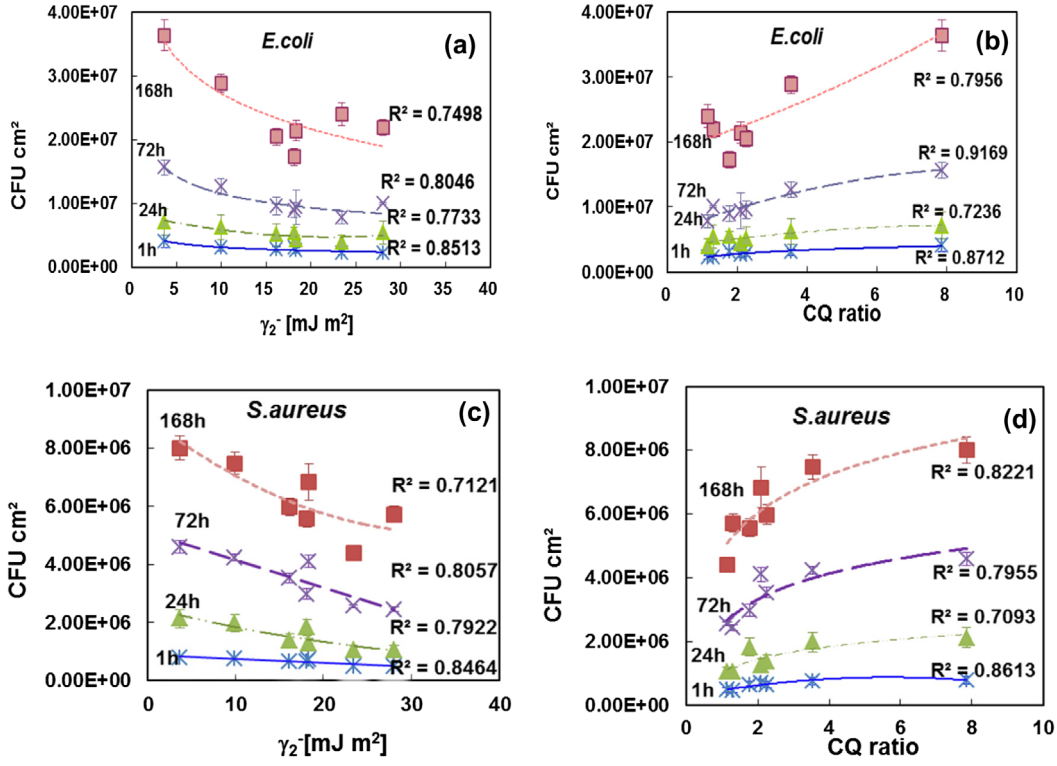

Figure 9. Effect of surface energy components γ_2^- and γ_2^{LW}/γ_2^- (CQ ratio) on the attachment of *E. coli* and *S. aureus* biofilms (N=15, error bars = SE).

for contact times of 1, 24, 72 and 168 h, respectively. The bacterial removal percentage increased with increasing the γ_2^- values of the coatings. Figure 10b and d show that the removal percentage of *E. coli* biofilm and *S. aureus* biofilm decreased with increasing the γ_2^{LW}/γ_2^- ratio. Again there was a good correlation between bacterial removal and the γ_2^{LW}/γ_2^- ratio.

4. Discussion

In general the antibacterial efficiency of Ag-based coatings depends mainly on the release rate of Ag ions (Fordham et al. 2014). The experimental results clearly indicate that the amounts of Ag ion release from all the Ag-TiO_2 coatings were much higher than that from the Ag coating. This finding explains why the Ag-TiO_2 coatings performed better than the Ag coating against bacterial adhesion, which was consistent with the results of Motlagh et al. (2014). In addition, the surface energy also plays an important role in bacterial adhesion (Yeo et al. 2012). In general, bacteria are negatively charged, and the larger the electron donor component γ_2^- of a surface, the more negatively charged the surface (Liu and Zhao 2011). Therefore, bacterial adhesion should decrease with increasing electron donor γ_2^-values of the coatings if other parameters that affect bacterial adhesion are identical (Liu and Zhao 2011). Table 4 indicates that the γ_2^- value of the Ag-TiO_2 coatings significantly increased due to the incorporation of TiO_2 nanoparticles

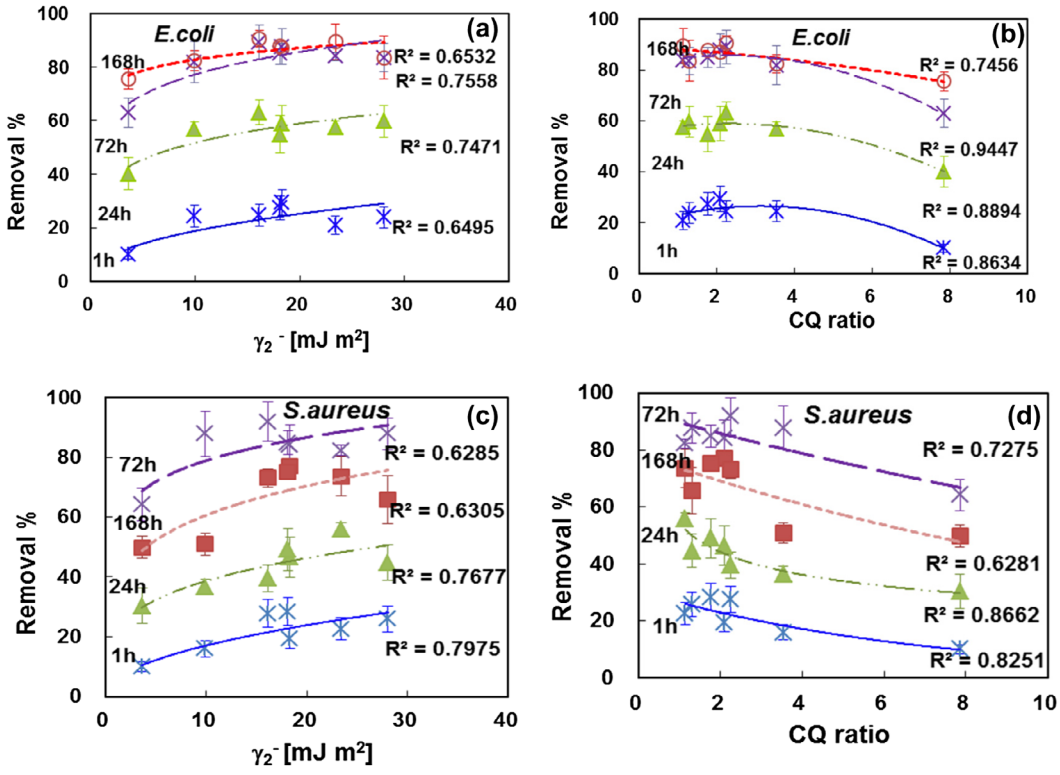

Figure 10. Effect of the surface energy components γ_2^- and γ_2^{LW}/γ_2^- on the removal of *E. coli* and *S. aureus* biofilms (N =15, error bars = SE).

into the Ag coatings. This means the incorporation of TiO_2 nanoparticles increases the negative charge of the Ag-TiO_2 coatings. As both *E. coli* and *S. aureus* cells are negatively charged, this further explains why the Ag-TiO_2 coatings were repellent to the bacteria and performed much better than the Ag coating or the Ti surface against bacterial adhesion. Figure 6 also indicates that the number of adhered *E. coli* cells was much higher than *S. aureus* cells. It has been reported that different surface energies cause different bacterial adhesion due to bacteria being repelled from the surface by charge similarities when coming closer to the surface (Liu et al. 2015). Table 4 shows that the γ_2^- value of *S. aureus* (21.33 mJ m^{-2}) is much higher than that of *E. coli* (10.31 mJ m^{-2}). This explains why the *S. aureus* is relatively more repellent to the coatings. Liu and Zhao (2011) demonstrated that the ratio of LW apolar to electron donor surface energy components of substrata (γ_2^{LW}/γ_2^-, the CQ ratio) controls bacterial attachment and removal using the extended DLVO theory. Figures 9 and 10 further demonstrate the relationship experimentally.

5. Conclusions

A range of Ag-TiO_2 nanocomposite coatings with different TiO_2 contents on a Ti substratum were successfully prepared using an electroless plating technique. The TiO_2 particles were homogenously incorporated in the Ag matrix. The TiO_2 content in the coatings increased with increasing TiO_2 concentration in the plating solution. This work demonstrated for the first time the mechanism of the synergistic effect of Ag-TiO_2 coatings on antibacterial efficiency. The incorporation of TiO_2 nanoparticles into an Ag matrix promoted Ag ion release and increased the electron donor (γ_2^-) surface energy of the coatings, leading to the enhanced antibacterial effect of the Ag-TiO_2 coatings. The experimental results indicate that bacterial adhesion or the percentage removal has strong correlation with γ_2^- or the CQ (γ_2^{LW}/γ_2^-) ratio. The number of adhered bacteria decreased with an increasing γ_2^- value or with a decreasing the CQ ratio. The results give a clear direction for the design of antibacterial coatings for orthopedic and dental application by using the highest γ_2^- value approach or the lowest CQ ratio approach.

Disclosure statement

No potential conflict of interest was reported by the authors.

Funding

Financial supports from the Scientific Research Common Program of Beijing Municipal Commission of Education

[grant number KM201510025008], the National Nature Science Foundation of China [51701131], the Internal Exchange Training of Teacher [07001160950171] and the UK Engineering and Physical Sciences Research Council [EP/P00301X/1] are acknowledged.

References

Ashkarran AA, Aghigh SM, Kavianipour M, Farahani NJ. 2011. Visible light photo-and bioactivity of Ag/TiO_2 nanocomposite with various silver contents. Curr Appl Phys. 11:1048–1055. doi: 10.1016/j.cap.2011.01.042.

Cotolan N, Rak M, Bele M, Cör A, Muresan LM, Milošev I. 2016. Sol-gel synthesis, characterization and properties of TiO_2 and Ag-TiO_2 coatings on titanium substrate. Surf Coat Technol. 307:790–799. doi: 10.1016/j.surfcoat.2016.09.082.

De Giglio E, Cafagna D, Cometa S, Allegretta A, Pedico A, Giannossa LC, Sabbatini L, Mattioli-Belmonte M, Iatta R. 2013. An innovative, easily fabricated, silver nanoparticle-based titanium implant coating: development and analytical characterization. Anal Bioanal Chem. 405:805–816. doi: 10.1007/s00216-012-6293-z.

Esfandiari N, Simchi A, Bagheri R. 2014. Size Tuning of Ag-decorated TiO_2 nanotube arrays for improved bactericidal capacity of orthopedic implants. J Biomed Mater Res A. 102:2625–2635. doi: 10.1002/jbm.a.v102.8.

Fordham WR, Redmond S, Westerland A, Cortes EG, Walker C, Gallagher C, Medina CJ, Waecther F, Lunk C, Ostrum RF, et al. 2014. Silver as a bactericidal coating for biomedical implants. Surf Coat Technol. 253:52–57. doi: 10.1016/j.surfcoat.2014.05.013.

Frandsen CJ, Noh K, Brammer KS, Johnston G, Jin S. 2013. Hybrid micro/nano-topography of a TiO_2 nanotube-coated commercial zirconia femoral knee implant promotes bone cell adhesion *in vitro*. Mater Sci Eng C Mater Biol Appl. 33:2752–2756. doi: 10.1016/j.msec.2013.02.045.

Guo R, Yin G, Sha X, Zhao Q, Wei L, Wang H. 2015. The significant adhesion enhancement of Ag–polytetrafluoroethylene antibacterial coatings by using of molecular bridge. Appl Surf Sci. 341:13–18. doi: 10.1016/j.apsusc.2015.02.131.

Gyorgyey A, Janovak L, Adam A, Kopniczky J, Toth LL, Deak A, Panayotov I, Cuisinier F, Dekany I, Turzo K. 2016. Investigation of the *invitro* photocatalytic antibacterial activity of nanocrystalline TiO_2 and coupled TiO_2/Ag containing copolymer on the surface of medical grade titanium. J Biomater Appl. 31:55–67. doi: 10.1177/0885328216633374.

Jia Z, Xiu P, Li M, Xu X, Shi Y, Cheng Y, Wei S, Zheng Y, Xi T, Cai H, Liu Z. 2016. Bioinspired anchoring AgNPs onto micro-nanoporous TiO_2 orthopedic coatings: trap-killing of bacteria, surface-regulated osteoblast functions and host responses. Biomaterials. 75:203–222. doi: 10.1016/j.biomaterials.2015.10.035.

Kim J, Lee S, Kim CM, Seo J, Park Y, Kwon D, Lee SH, Yoon TH, Choi K. 2014. Non-monotonic concentration–response relationship of TiO_2 nanoparticles in freshwater cladocerans under environmentally relevant UV-A light. Ecotox Environ Safe. 101:240–247. doi: 10.1016/j.ecoenv.2014.01.002.

Kuo YL, Chen HW, Ku Y. 2007. Analysis of silver particles incorporated on TiO_2 coatings for the photodecomposition of o-cresol. Thin Solid Films. 515:3461–3468. doi: 10.1016/j.tsf.2006.10.085.

Motlagh AL, Bastani S, Hashemi MM. 2014. Investigation of synergistic effect of nano sized Ag/TiO_2 particles on antibacterial, physical and mechanical properties of UV-curable clear coatings by experimental design. Prog Org Coat. 77:502–511. doi: 10.1016/j.porgcoat.2013.11.014.

Li B, Logan BE. 2005. The impact of ultraviolet light on bacterial adhesion to glass and metal oxide-coated surface. Colloids Surf B Biointerfaces. 41:153–161. doi: 10.1016/j.colsurfb.2004.12.001.

Li NN, Li GL, Wang HD, Kang JJ, Dong TS, Wang HJ. 2015. Influence of TiO_2 content on the mechanical and tribological properties of Cr_2O_3-based coating. Mater Des. 88:906–914. doi: 10.1016/j.matdes.2015.09.085.

Liu C, Zhao Q. 2011. Influence of surface-energy components of Ni–P–TiO_2–PTFE nanocomposite coatings on bacterial adhesion. Langmuir. 27:9512–9519. doi: 10.1021/la200910f.

Liu WW, Su PL, Chen S, Wang N, Wang JS, Liu YR, Ma YP, Li HY, Zhang ZT, Webster TJ. 2015. Antibacterial and osteogenic stem cell differentiation properties of photoinduced TiO_2 nanoparticle-decorated TiO_2 nanotubes. Nanomedicine. 10:713–723. doi: 10.2217/nnm.14.183.

Matsunaga T, Tomoda R, Nakajima T, Wake H. 1985. Photoelectrochemical sterilization of microbial cells by semiconductor powders. FEMS Microbiol Lett. 29:211–214. doi: 10.1111/fml.1985.29.issue-1-2.

Prakash J, Kumar P, Harris RA, Swart C, Neethling JH, van Vuuren AJ, Swart HC. 2016. Synthesis, characterization and multifunctional properties of plasmonic Ag-TiO_2 nanocomposites. Nanotechnology. 27:355707–355726. doi: 10.1088/0957-4484/27/35/355707.

Sulej-Chojnacka J, Kloskowski T, Borowski J, Ignatev M, Bajek A, Wisniewska-Weinert H, Kwiecinska-Pirog J, Drewa T. 2016. Prototype coatings of titanium alloy samples with silver nanoparticles and their niological characterization, *in vitro* study. J Biomater Tiss Eng. 6:463–472. doi: 10.1166/jbt.2016.1469.

van Oss CJ. 1994. Interfacial forces in aqueous media. New York (NY): Marcel Dekker.

Yeo IS, Kim HY, Lim KS, Han JS. 2012. Implant surface factors and bacterial adhesion: a review of the literature. Int J Artif Organs. 35:762–772. doi: 10.5301/ijao.5000154.